The Molecular Structures, Energetics, and Nature of Interactions in Ar n −N 2 H + (n = 1−12) Complexes

ARTICLE *in* THE JOURNAL OF PHYSICAL CHEMISTRY A · NOVEMBER 2002

Impact Factor: 2.69 · DOI: 10.1021/jp0207984

5 AUTHORS, INCLUDING:

Yinghong Sheng
Florida Gulf Coast University
35 PUBLICATIONS **408** CITATIONS

The Molecular Structures, Energetics, and Nature of Interactions in Ar_n-N_2H^+ ($n = 1-12$) Complexes

Yinghong Sheng,[†] Robert W. Gora,[†,‡] Szczepan Roszak,[†,‡] Malgorzata Kaczorowska,[†] and Jerzy Leszczynski*[,†]

The Computational Center for Molecular Structure and Interactions, Department of Chemistry, Jackson State University, P.O. Box 17910, J.R. Lynch Street, Jackson, Mississippi 39217, and Institute of Physical and Theoretical Chemistry, Wroclaw University of Technology, Wyb. Wyspianskiego 27, 50-370 Wroclaw, Poland

Received: March 25, 2002; In Final Form: September 3, 2002

The results of theoretical studies on structures and energetics are presented for the proton-bound complexes Ar_n-N_2H^+ ($n = 1-12$). Complexes are formed due to the consecutive filling of shells. The largest studied cation possesses the slightly deformed icosahedral geometry. For shells formed outside the Ar-N_2H^+ core, increasing binding energies are observed during the coordination of consecutive Ar atoms. Such an anomalous behavior is also observed for consecutive values of enthalpy and entropy of ligand binding, Mulliken atomic charges, and Ar−H^+ stretching vibrations. The analysis of physical components resulting from interaction energy decomposition allows the observed phenomenon to be rationalized.

I. Introduction

The solvation of cations with neutral ligands has recently been a subject of extensive studies due to the importance of such processes in chemistry, physics, and biology.[1−3] An important role is played by proton-bound complexes.[4] Despite its relative simplicity, such complexes are not well understood, and the nature of interactions still has to be carefully investigated. The energetics and dynamics of reactions leading to the proton-bound complexes are sensitively dependent upon the cluster size.[5−9] A detailed understanding of the interplay between the ion−ligand and ligand−ligand interactions is required to rationalize the chemistry of these clusters. The determination of the balance between ionic and covalent components of the interactions between the core cation and ligand atoms or molecules may lead to the possible explanation for observed structural changes.[10] Another cause for enforcing the particular geometry are ligand−ligand interactions.[7] The discovered anomalous change of bond energies in $(H_2)_n$-N_2H^+ cluster ions[5] leads to the question of the generality of such a phenomenon.

The interactions of cations with noble gas atoms produce complexes in which the core−ligand interactions are an order of magnitude larger than the corresponding ligand−ligand interactions. However, a detailed study on the Ar_n-HCO^+ moieties[7] suggests that ligand−ligand interactions may still be the force governing the topology of complexes. Due to differences between atomic electronegativities, the interaction energies in Ar_n-HCO^+ and Ar_n-N_2H^+ complexes also differ significantly,[7] and conclusions drown from the study of one system may not apply to the other. The majority of data concerning Rg_n-N_2H^+ (Rg = He, Ne, Ar) moieties is available from infrared spectra.[6,11−16] Some useful information also comes[5] from the mass spectrometric experiment for the $(H_2)_n$-N_2H^+ ion. The ab initio studies are restricted to Rg···N_2H^+ (Rg = He, Ne, Ar) dimers.[13,14,16,17] The simple modeling of structures and spectra based on the rigid monomer interaction potentials is also available for some cases.[13,17−20]

The present work addresses Ar_n-N_2H^+ ($n = 1-12$) cationic clusters. Ab initio studies are presented for structures, thermodynamics, and infrared spectra of complexes. A detailed analysis concerning the nature of interactions involved in the cluster formation sheds new light on the characterization of bonding observed in proton-bound complexes.

II. Theoretical Approach and Computational Details

The geometries of studied species were optimized applying the second-order Møller−Plesset perturbation theory (MP2).[21] No symmetry constraints were imposed during the optimization process, and the geometry searches were carried out for a number of possible isomers to ensure the location of the global minimum. Additionally, single point calculations were performed within the coupled cluster method with single and double substitutions and including triple excitations noniteratively (CCSD(T)).[22] All the results presented in this study have been obtained using the standard triple-ζ valence basis set supplemented with diffuse and polarization functions (6-311+G-(d,p)).[23] The selected medium size basis set was the largest feasible basis set for studied complexes. The basis set of this size leads to geometries of semiquantitative quality. The calculated polarizability (MP2) of the Ar atom (8.64 a_0^3) reasonably reproduces its experimental value (11.08 a_0^3).[26] Theoretical methods combined with the assumed basis set ensure the reasonable representation of interactions within the cluster, including induction and dispersion forces which are difficult to reproduce. For smaller size clusters, MP2 calculations were performed applying aug-cc-pVDZ and aug-cc-pVTZ basis sets.[24,25] These collections reproduce 88% and 97% of the experimental polarizability of the Ar atom and should give reliable interaction energies. The G2(MP2) scheme[27] was also applied for complexes with the number of Ar atoms less than 6. Vibrational frequencies and thermodynamic properties of the studied complexes were calculated applying the ideal gas, rigid rotor, and harmonic oscillator approximations.[28]

[†] Jackson State University.
[‡] Wroclaw University of Technology.

10.1021/jp0207984 CCC: $22.00
Published on Web 10/17/2002

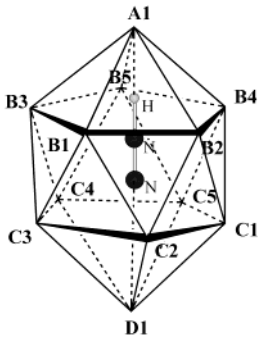

Figure 1. Consecutive filling positions of Ar atoms around the N_2H^+ core in the Ar_n-N_2H^+ complex.

The total interaction energy calculated at the MP2 level:

$$\Delta E_{MP2} = E_{AB} - E_A - E_B \quad (1)$$

has been decomposed

$$\Delta E_{MP2} = \Delta E_{SCF} + \epsilon_{MP}^{(2)} \quad (2)$$

into the Hartree−Fock and correlation components. The applied SCF energy decomposition was performed within the variational−perturbational scheme, corrected for the basis set superposition error.[29] In the above scheme, ΔE_{SCF} was partitioned into the electrostatic ($\epsilon_{el}^{(10)}$) and Heitler−London exchange (ϵ_{ex}^{HL}) first-order components and the higher order delocalization (ΔE_{del}^{HF}) term. The delocalization energy accounts for the charge transfer, induction, and other higher order Hartree−Fock terms.[30] The main contribution to the correlation energy $\epsilon_{MP}^{(2)}$ is due to the second-order Hartree−Fock dispersion energy ($\epsilon_{disp}^{(20)}$). The remaining terms, giving significant contribution to $\epsilon_{MP}^{(2)}$, are correlation corrections to SCF components.[31]

The calculations were carried out using the Gaussian 98 suite of codes.[32] The interaction energy decomposition was performed applying the modified version[33] of the Gamess program.[4]

III. Results and Discussion

A. Structures of Complexes. The optimized structures of the Ar_n-N_2H^+ ($n = 1-12$) complexes, following the pattern of filling four (A−D) consecutive shells, are shown in Figure 1. Figure 2 displays the obtained geometries of all considered species. Only a single isomer for the Ar-N_2H^+ complex has been located. The calculated bond distances (Table 1) agree well with other theoretical data.[6,16] More importantly, an analysis of the ground-state rotational constants leads to the center-of-mass separation[21] which is in good agreement with ab initio values presented in previous studies.[11]

The coordination of the second Ar atom destroys slightly the linear symmetry of the Ar-H^+-N_2 fragment (the Ar-H^+-N angle amounts to 177.1°). It is the first particle occupying the second shell (B), which is located on the plane perpendicular to the Ar-H^+-N_2 axes (Figure 1). The plane defining shell B divides the N−H^+ bond into two almost equal parts. The Ar(A1)−Ar-(B1) distance (Table 1) is close to the bond length of the Ar_2 dimer. The addition of the third atom (second to the B shell) leads to C_s geometry for Ar_3-N_2H^+. The separation of argon atoms in the B shell is again close to the Ar_2 bond distance, indicating the stabilizing effect of ligand−ligand interactions. This bonding pattern is continued in Ar_4-N_2H^+ and Ar_5-N_2H^+. These complexes also possess C_s symmetry, suggesting that the occupation of the B shell is driven by the Ar−Ar interactions. The studied structures for $n = 1-4$ are similar to those determined for their Ar_n-HCO^+ analogues.[7] Unfortunately, the geometry search in the case of the Ar_5−HCO^+ complex has been performed with an a priori assumption of C_{4v} symmetry, and it is difficult to judge if this assumption was justified. Another related C^+Ar_4 complex,[35] which has been considered, possesses the planar D_{4h} structure, indicating that in same cases the core−argon interactions control the overall topology of the cluster. The MP2 calculations using the aug-cc-pVTZ basis set reveal that the Ar_5-N_2H^+ complex with the C_{4v} complex is 0.004 kcal/mol less stable than the C_s structure. The vibrational frequencies calculated at the MP2/aug-cc-pVDZ level indicate that both geometries located represent true minima. These isomers are separated by the transition state with the geometry being an intermediate structure between true energy minimum isomers. The activation barrier amounts to only 0.015 kcal/mol. Such a shallow potential barrier allows for long deflections from the equilibrium positions. The small energy difference between the two isomers of Ar_5-N_2H^+ leads to the conclusion that Ar atoms can move almost freely along the B ring. Because of the values of van der Waals radii of Ar, the ring defining the B shell cannot host five atoms without relaxing the optimal H^+−Ar distances. Analogous to $(H_2)_5$-N_2H^+, assuming that the proton's coordination number is 6, Dopfer et al. suggested that the preferred isomer should be the one characterized by A(1)B-(4)C(1) occupation. Our calculations indicate, however, that the energetically lowest complex possesses five atoms in the B shell despite the necessity to enlarge the radius of the B ring. The MP2/aug-cc-pVTZ calculations indicate that the A(1)B(5) complex is more stable then its A(1)B(4)C(1) isomer with the energy difference of 0.83 kcal/mol. The C_{5v} complex was also determined as the preferred structure for the Ar_6-HCO^+ cation.[7] Similar to the findings reported for the Ar_n-HCO^+ complexes, the conclusion may be drawn of the significant influence of Ar−Ar interactions on the position of the subsequent Ar atoms.[7] The bond angle of 100.1° between three Ar atoms in shell B for the Ar_4-N_2H^+ cluster supports the interpretation of studied complexes (up to $n = 5$) as species representing cubic crystal structures of solid argon. The pattern continues for Ar_5-HN_2^+ (considering the C_{4v} isomer). The C_{5v} structure of Ar_6-N_2H^+ may only be formed in the noncrystal environment.

A third solvation ring (C) is formed due to the further coordination of argon atoms to Ar_6-N_2H^+. The shell is located on the plane below the terminal N atom (Figure 1). The distance from the center of this five-membered ring to the terminal nitrogen is about 1.5 Å, and the separation between B and C solvation rings amounts to 3.3 Å. The Ar−Ar distances within the C shell decrease from 3.99 Å in the A(1)B(5)C(2) complex to 3.68 Å in the A(1)B(5)C(5) complex. Every Ar atom introduced into the C shell interacts with atoms from the B shell and distorts the structure of this ring. The solvation of the N_2H^+ ion is completed by the coordination of the 12th Ar atom. The Ar_{12}-N_2H^+ complex possesses slightly distorted icosahedral geometry (Figure 1), with two Ar atoms nested on the N_2H^+ axis (on both sides of the H^+ and N terminal positions) and two five-membered solvation rings around the linear core fragment.

B. Thermodynamics. The energies of ligand coordination to the charged core usually decrease as a function of the size of the complex.[36] The binding capability of the charged fragment in the larger complex is smaller due to its reduced charge as an effect of the charge transfer from (or to) consecutive ligands. However, as discovered in the case of $(H_2)_n$-N_2H^+, the successive attachment of H_2 molecules increases binding energies for

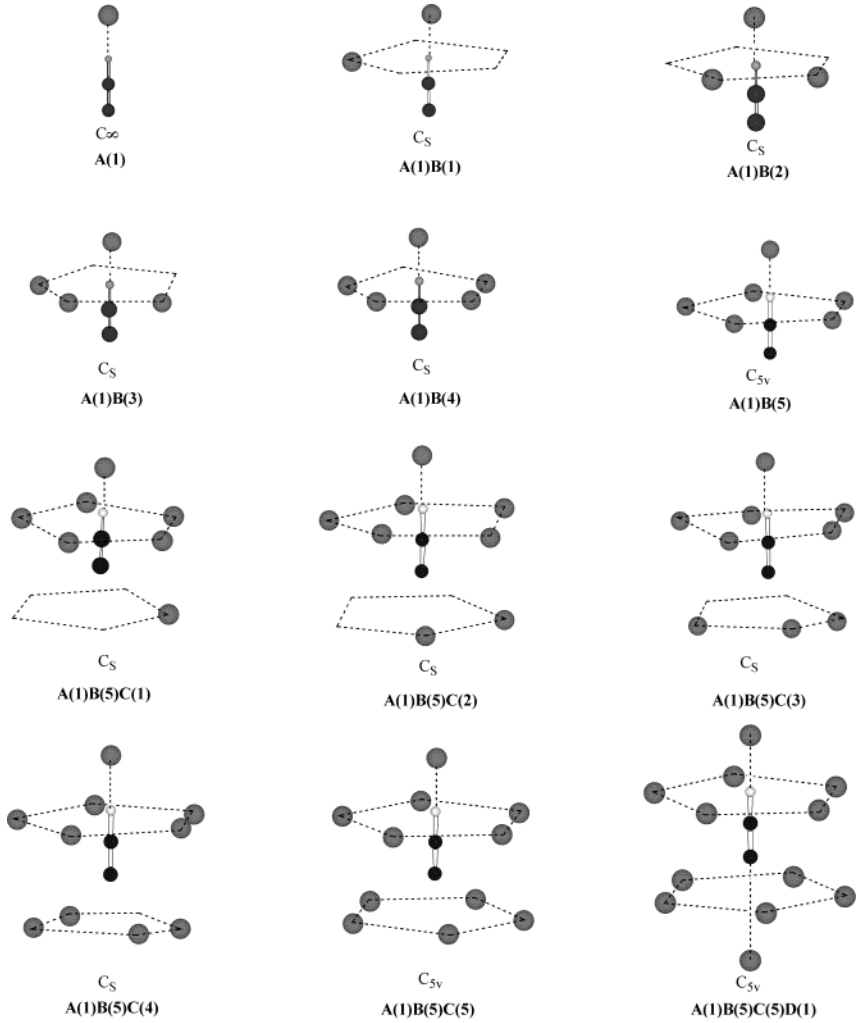

Figure 2. Optimized structures for Ar_n-N_2H^+ ($n = 1-12$) complexes. Geometrical parameters are given in Table 1.

incoming ligands.[5] A similar phenomenon has also been observed in the theoretical studies for Ar_n-HCO^+ complexes.[7]

The accurate reproduction of properties of the dissociation reaction Ar_n-$N_2H^+ = Ar_{n-1}$-$N_2H^+ + Ar$ requires the extended basis set which is not very sensitive to the counterpoise correction problem. The dissociation energy of Ar-N_2H^+ calculated within the MP2/aug-cc-pVTZ level of theory leads to $D_o = 7.93$ kcal/mol, which is in excellent agreement with the experimental value of 7.95 kcal/mol. The dissociation energies for Ar_n-N_2H^+ ($n = 1-6$) complexes determined using the extended aug-cc-pVDZ and aug-cc-pVTZ basis sets are reported in Table 2. However, our medium-sized basis set, which allows the same level calculations to be performed even for the largest considered complex, reasonably reproduces the experimental value of the dissociation energy of the Ar-N_2H^+ dimer, and the calculations of larger systems should reveal proper trends during the reaction of the cluster formation. The predicted consecutive dissociation energies of Ar_n-N_2H^+ complexes clearly indicate the formation of four distinctive shells (Table 2).

The filling of the B shell for some clusters leads to an increase of the consecutive stabilization energy. This observation agrees with the similar pattern discovered in mass spectrometry measurements performed for $(H_2)_n$-N_2H^+ ($n = 2-5$) clusters. It should be noted that the entropy is determined from frequencies calculated in harmonic approximation and therefore should be treated with caution. However, it may be useful for qualitative considerations. The calculated consecutive entropy changes are indicative of the higher rigidity of enlarged complexes with the clear shell closing for the A(1)B(5) occupation (Table 2). The formation of the C shell proceeds according to the same pattern with the optimal shell occupation for the A(1)B(5)C(4) isomer. As shown by the incremental entropy values, the shell closes for the five Ar atoms occupying the C shell. The addition of the 12th argon atom enhances the overall stabilization of the structure.

C. Nature of Interactions. The Mulliken population analysis indicates a significant charge transfer from argon ligands to the N_2H^+ core fragment. The atomic charge distribution agrees well with the pattern found in structures and the thermodynamic data (Table 3). Interestingly, the average electronic density per Ar atom transferred to the Ar-N_2H^+ core slightly increases for the higher occupation of the B shell. Such behavior responding to the repulsion of Ar electronic shells is anomalous considering previous findings.[8,9] It may be considered as a forecast of anomalous behavior in binding energies. Despite this interesting behavior, the findings of the charge distribution studied within the population analysis should be treated with caution due to the known qualitative character of this theoretical tool.

The anomalous change of binding energies within B and C shells, discussed in the previous section, is a consequence of two-body forces that act between the components of the complexes. The three-body interactions calculated for the dissociation reaction Ar_3-$N_2H^+ =$ Ar-$N_2H^+ +$ Ar + Ar amount to 0.3% of the total interaction energy related to the formation of the B shell. The dominant role of two-body interactions is also found in heavier complexes. The binding energy of argons

TABLE 1: Bond Lengths and Ar−Ar Distances for Optimized Structures of Ar_n-HN_2^+ (n = 1−12) Complexes (Distances in Å)

Core Structural Parameters and Ar−Ar Distances between A and B Shells

complex structure	N-N	H^+-N	A1-H^+	A1-B1	A1-B2	A1-B3	A1-B4	A1-B5
A(1)	1.116	1.088	1.839					
A(1)B(1)	1.115	1.086	1.846	3.897				
A(1)B(2)	1.116	1.084	1.846	3.947	3.945			
A(1)B(3)	1.115	1.081	1.863	3.917	3.992	3.918		
A(1)B(4)	1.115	1.080	1.869	3.912	3.976	3.979	3.913	
A(1)B(5)	1.115	1.078	1.871	4.005	4.001	4.004	4.006	4.002
A(1)B(5)C(1)	1.115	1.077	1.872	4.018	4.017	3.997	4.013	4.018
A(1)B(5)C(2)	1.115	1.077	1.875	3.900	4.085	4.022	3.896	4.021
A(1)B(5)C(3)	1.115	1.076	1.883	4.043	3.939	3.857	3.909	4.072
A(1)B(5)C(4)	1.115	1.073	1.885	3.953	3.878	3.937	3.945	3.883
A(1)B(5)C(5)	1.115	1.074	1.888	3.934	3.927	3.931	3.939	3.932
A(1)B(5)C(5)D(1)	1.116	1.073	1.904	3.816	3.818	3.812	3.816	3.812

Distances between Proton and Ar Atoms of B Shell

	H^+-B1	H^+-B2	H^+-B3	H^+-B4	H^+-B5
A(1)					
A(1)B(1)	3.230				
A(1)B(2)	3.225	3.222			
A(1)B(3)	3.245	3.222	3.245		
A(1)B(4)	3.250	3.249	3.249	3.250	
A(1)B(5)	3.291	3.292	3.296	3.296	3.295
A(1)B(5)C(1)	3.305	3.297	3.303	3.293	3.291
A(1)B(5)C(2)	3.243	3.293	3.311	3.244	3.311
A(1)B(5)C(3)	3.273	3.238	2.341	3.318	3.230
A(1)B(5)C(4)	3.249	3.220	3.239	3.226	3.245
A(1)B(5)C(5)	3.231	3.225	3.229	3.231	3.226
A(1)B(5)C(5)D(1)	3.220	3.220	3.220	3.220	3.220

Distances between Argon Atoms Occupying B and C Shells

	B1-B2	B2-B4	B4-B5	B1-B3	B3-B5	C1-C2	C2-C3	C3-C4	C4-C5	C1-C5	D1-C
A(1)B(2)	4.115										
A(1)B(3)	4.035	4.033									
A(1)B(4)	3.994	4.001	4.001								
A(1)B(5)	3.836	3.836	3.837	3.836	3.836						
A(1)B(5)C(1)	3.839	3.822	3.837	3.849	3.847	3.966					
A(1)B(5)C(2)	3.833	3.833	3.822	3.823	3.823	3.989	3.907				
A(1)B(5)C(3)	3.831	3.775	3.801	3.824	3.819	3.947	3.831	3.860			
A(1)B(5)C(4)	3.796	3.775	3.740	3.841	3.774	3.677	3.684	3.680	3.678	3.689	
A(1)B(5)C(5)	3.777	3.761	3.763	3.765	3.789	3.722	3.721	3.715	3.717	3.720	
A(1)B(5)C(5)D(1)	3.773	3.773	3.783	3.784	3.788	3.737	3.738	3.744	3.739	3.749	3.897

Distances between Terminal N Atom and Ar Atoms of the C Shell

	N-C1	N-C2	N-C3	N-C4	N-C5
A(1)B(5)C(1)	3.361				
A(1)B(5)C(2)	3.343	3.340			
A(1)B(5)C(3)	3.287	3.323	3.285		
A(1)B(5)C(4)	3.269	3.305	3.321	3.282	
A(1)B(5)C(5)	3.466	3.499	3.469	3.484	3.442
A(1)B(5)C(5)D(1)	3.401	3.401	3.401	3.402	3.401

in the B shell is higher by approximately 1 kcal/mol compared to interactions within the C shell. Although isomers with mixed partial filling of shells (e.g., A(1)B(2)C(1) complex) are possible, their presence is less probable due to the unfavorable thermodynamics.

The interaction energy decomposition provides more detailed information concerning the nature of forces leading to the cluster formation (Table 4). The final structure of complexes is established due to the interplay between the electrostatic and covalent interactions of the core and ligands and among ligands. The electrostatic interactions are expected to lead to the most symmetrical geometries (C_{2v}, C_{3v}, and C_{4v} for n = 3, 4, and 5, respectively) in order to minimize the exchange repulsion between Ar atoms.[10] The covalent contribution, including ΔE_{del}^{HF} (containing mainly induction and charge-transfer energies) and $\epsilon_{disp}^{(20)}$ interactions, favors the structures which maximize the overlap of π orbitals of the N−N−H^+ core with orbitals of Ar atoms. Geometries driven by covalent forces would then favor C_s symmetry with the Ar−H^+−Ar angle close to 90°. The additional factors, which should be taken into account, are direct Ar−Ar interactions contributing to the stabilization.

The interaction energy partitioning indicates (Table 4) that clusters are formed mainly due to the correlation forces. The Hartree−Fock interactions lead to unstable structures. The energy decomposition terms follow the shell development; however, their functional behavior within a shell is different for the particular interaction energy component studied. Consecutive electrostatic ($\epsilon^{el(10)}$) and correlation ($\epsilon_{MP}^{(2)}$) contributions increase with the progress in the shell occupation, while the delocalization energy (ΔE_{del}^{HF}), although attractive, is almost constant for every additional Ar atom coordinated. All attractive forces are balanced by the faster growing exchange repulsion (ϵ_{ex}^{HF}). The overall interaction energy (ΔE_{MP}^{2}), being the

TABLE 2: Calculated Consecutive Dissociation Energies, Enthalpies, and Entropies for the Reaction Ar_n-N_2H^+ = Ar_{n-1}-N_2H^+ + Ar (All Values in kcal/mol)

		MP2						G2MP2	CCSD(T)	expt[c]
n	shell structure	D_e	D_0	ΔH	ΔS	D_e[a]	D_e[b]	D_e	D_e	D_0
1	A(1)	7.70	6.44	7.16	17.52	8.24	9.19	5.51	7.61	7.95
2	A(1)B(1)	1.48	1.11	1.13	14.76	2.44	2.73	2.17	1.43	
3	A(1)B(2)	2.03	1.80	1.67	17.70	2.79	3.02	2.57	1.98	
4	A(1)B(3)	2.07	1.88	1.73	17.89	2.73	2.94	2.51	2.02	
5	A(1)B(4)	2.24	2.11	1.96	18.38	2.80	2.96	2.55	2.19	
6	A(1)B(5)	2.44	2.23	2.13	21.42	2.66	2.79	2.33	2.40	
7	A(1)B(5)C(1)	1.45	1.32	1.13	16.02					
8	A(1)B(5)C(2)	1.78	1.60	1.48	20.12					
9	A(1)B(5)C(3)	1.95	1.72	1.62	15.60					
10	A(1)B(5)C(4)	2.18	1.98	1.88	22.15					
11	A(1)B(5)C(5)	1.44	1.17	1.15	29.19					
12	A(1)B(5)C(5)D(1)	2.41	2.88	3.53	30.30					

[a] Calculations in aug-cc-pVDZ basis set. [b] Calculations in aug-cc-pVTZ basis set. [c] Reference 11.

TABLE 3: Atomic Charge from the Mulliken Population Analysis Performed at the MP2/6-311+g(d,p) Level of Theory

	argon atoms															
shell structure	N_{end}	N	H^+	N_2H^+	A1	B1	B2	B3	B4	B5	C1	C2	C3	C4	C5	D1
A(1)	−0.062	0.467	0.380	0.785	0.215											
A(1)B(1)	0.017	0.341	0.432	0.790	0.195	0.015										
A(1)B(2)	0.009	0.314	0.434	0.758	0.196	0.023	0.023									
A(1)B(3)	0.014	0.284	0.433	0.730	0.196	0.022	0.031	0.022								
A(1)B(4)	0.043	0.236	0.422	0.702	0.194	0.030	0.030	0.022	0.022							
A(1)B(5)	−0.036	0.262	0.381	0.664	0.198	0.028	0.028	0.028	0.028	0.028						
A(1)B(5)C(1)	−0.092	0.291	0.384	0.584	0.222	0.036	0.036	0.035	0.035	0.036	0.017					
A(1)B(5)C(2)	−0.111	0.285	0.385	0.623	0.200	0.029	0.030	0.028	0.029	0.028	0.016	0.016				
A(1)B(5)C(3)	−0.211	0.344	0.384	0.625	0.190	0.029	0.029	0.028	0.030	0.029	0.014	0.015	0.014			
A(1)B(5)C(4)	−0.263	0.359	0.383	0.572	0.203	0.031	0.032	0.031	0.030	0.029	0.018	0.017	0.019	0.017		
A(1)B(5)C(5)	−0.162	0.251	0.385	0.550	0.200	0.032	0.032	0.032	0.032	0.032	0.018	0.018	0.018	0.018	0.018	
A(1)B(5)C(5)D(1)	−0.450	0.505	0.399	0.530	0.207	0.031	0.031	0.031	0.031	0.031	0.017	0.017	0.017	0.017	0.017	0.024

TABLE 4: Interaction Energy Decomposition for Energetically Favored Consecutive Filling of Shells in Ar_n-N_2H^+ (n = 1−12) Complexes[a]

system	shell occupation	$\epsilon_{el}^{(10)}$	ϵ_{ex}^{HL}	ΔE_{del}^{HF}	ΔE_{SCF}	$\epsilon_{disp}^{(20)}$	$\epsilon_{MP}^{(2)}$	ΔE_{MP2}
N_2H^+ + Ar	A(1)	−0.06	13.22	−16.58	−3.41	−2.67	−2.92	−6.33
Ar-N_2H^+ + Ar	A(1)B(1)	−0.27	1.13	−1.01	−0.15	−0.62	−0.60	−0.74
Ar_2-N_2H^+ + Ar	A(1)B(2)	−0.30	1.31	−1.06	−0.05	−0.67	−0.73	−0.78
Ar_3-N_2H^+ + Ar	A(1)B(3)	−0.32	1.37	−1.03	0.02	−0.69	−0.74	−0.73
Ar_4-N_2H^+ + Ar	A(1)B(4)	−0.35	1.49	−1.03	0.11	−0.73	−0.79	−0.69
Ar_5-N_2H^+ + Ar	A(1)B(5)	−0.45	1.82	−1.01	0.37	−0.85	−0.93	−0.56
Ar_6-N_2H^+ + Ar	A(1)B(5)C(1)	−0.24	0.94	−0.51	0.19	−0.52	−0.51	−0.33
Ar_7-N_2H^+ + Ar	A(1)B(5)C(2)	−0.32	1.26	−0.55	0.39	−0.67	−0.65	−0.28
Ar_8-N_2H^+ + Ar	A(1)B(5)C(3)	−0.35	1.41	−0.58	0.47	−0.70	−0.74	−0.27
Ar_9-N_2H_+ + Ar	A(1)B(5)C(4)	−0.47	1.78	−0.57	0.74	−0.80	−0.91	−0.17
Ar_{10}-N_2H^+ + Ar	A(1)B(5)C(5)	−0.61	2.14	−0.50	1.04	−0.80	−0.95	0.09
Ar_{11}-N_2H^+ + Ar	A(1)B(5)C(5)D(1)	−0.43	1.59	−0.30	0.87	−0.95	−	−0.08

[a] All values are given in kcal/mol.

balance of all decomposition terms, decreases slowly as a function of the occupation of shells. The "normal" behavior of total interaction energies, compared to anomalous binding energies, emphasizes the importance of the geometrical relaxation of formed species.

D. Vibrational Properties. A study of harmonic vibrational frequencies provides information concerning the structure of the core and also enhances the description of the properties of shellvent species.[37] The observed spectral shifts indicate their systematic dependence on the cluster size and provide indirect information concerning the cluster structures and relative stabilities of the isomers. Intramolecular stretching vibrations were determined experimentally for the Ar-N_2H^+ complex.[16] The ν_1 and ν_2 vibrations are located at 2505.5 and 2041.2 cm^{-1}, respectively, and were found to be mixed modes, both with large anharmonicity contributions. Calculated harmonic frequencies reproduce reasonably (2635.9 and 2020.6 cm^{-1}) the measured values, and may be accepted for qualitative considerations. The calculated N−H stretching vibrations (Table 5) follow the observed pattern of the cluster growth.[6] The experimental and theoretical data demonstrate that the dimer has a linear proton-bound configuration. The coordination of the first Ar to N_2H^+

TABLE 5: Calculated Harmonic Vibrational Frequencies (cm^{-1}) and IR Intensities (KM/mol, in Parentheses) for Vibration Modes Corresponding to the Ar-N_2H^+ Fragment of Ar_n-N_2H^+ Clusters

shell structure	N−H stretching ν_1	N−N stretching ν_2	Ar−H stretching ν_3
N_2H^+	3410.4*(655.7)*	2131.9*(3.4)*	
A(1)	2635.9*(2514.3)*	2020.6*(773.9)*	193.7*(84.7)*
A(1)B(1)	2658.4*(2433.8)*	2028.9*(672.4)*	192.2*(80.5)*
A(1)B(2)	2686.3*(2344.8)*	2038.3*(565.6)*	192.3*(74.3)*
A(1)B(3)	2707.1*(2255.7)*	2044.3*(497.4)*	191.5*(64.3)*
A(1)B(4)	2731.5*(2176.6)*	2049.7*(437.9)*	185.7*(63.4)*
A(1)B(5)	2747.7*(2115.2)*	2051.7*(397.9)*	183.9*(62.7)*
A(1)B(5)C(1)	2749.6*(2157.5)*	2052.9*(397.4)*	185.6*(64.3)*
A(1)B(5)C(2)	2761.5*(2180.4)*	2055.8*(377.8)*	184.7*(65.1)*
A(1)B(5)C(3)	2771.6*(2211.6)*	2057.3*(356.4)*	183.2*(66.0)*
A(1)B(5)C(4)	2793.3*(2237.8)*	2062.4*(328.2)*	184.5*(66.9)*
A(1)B(5)C(5)	2797.7*(2177.3)*	2059.7*(331.4)*	180.7*(63.1)*
A(1)B(5)C(5)D(1)	2810.8*(2173.9)*	2061.7*(296.2)*	171.7*(63.4)*

significantly lowers the ν_1 vibration. Further Ar ligands cause the ν_1 frequencies to shift to the blue. The perturbation in the energetics when going from A(1)B(4) and A(1)B(5) complexes, as well as shell closing, is quite visible as irregular changes of $\Delta\nu_1$. The stretching mode for the N−N bond follows the similar pattern. The Ar−H^+ stretching vibration shifts to the blue as a function of the shell occupation in both subsets corresponding to outer B and C shells. Such a variation correlates well with the anomalous change in binding energies.

IV. Conclusions

Despite their relative simplicity, proton-bound complexes are not well understood. The energetics and dynamics of reactions leading to the formation of complexes depend significantly on the cluster size. The successive clusters are formed by the filling of shells which leads to the largest Ar_{12}-N_2H^+ cluster of the distorted icosahedral geometry (Figure 1). Two shells hosting a single Ar atom (A, D) are located on the axes of the N_2H^+ core. Two others (B, C) form rings on planes perpendicular to Ar-N_2H^+. Molecular structures for clusters with shells that are not fully filled are always characterized by C_s symmetry with distances between Ar atoms being close to the bond of the Ar_2 dimer. The complete occupation of shells leads to the perfect C_{5v} geometries.

The consecutive binding energies and enthalpies of the Ar atom within the B and C shells increase with higher occupation. Such an anomalous behavior is rationalized on the basis of variations of Mulliken charges. The nature of binding is similar in the B and C shells. The calculated consecutive entropies for reactions of cluster formation are indicative of the shell closings leading to the largest complex of A(1)B(5)C(5)D(1). The interaction energy partitioning indicates that clusters are formed mainly due to the correlation forces. The regular pattern of total interaction energies, compared to anomalous binding energies, emphasizes the importance of the geometrical relaxation of the formed clusters. The blue shift of the Ar−H^+ stretching vibrations as a function of the occupation of the B and C shells correlates with the anomalous variation of the Ar binding energies.

Acknowledgment. This work was facilitated in part by NSF CREST Grants 9805465 and 9706268, ONR Grant N00014-98-1-0592, a Wroclaw University of Technology grant, and a grant from the Foundation for Polish Science (R.W.G.), and by the Army High Performance Computing Research Center under the auspices of the Department of the Army, Army Research Laboratory Cooperative Agreement DAAH04-95-2-0003/Contract DAAH04-95-C-0008. This work does not necessarily reflect the policy of the government, and no official endorsement should be inferred. We thank the Mississippi Center for Supercomputing Research, the Poznan and Wroclaw Supercomputing and Networking Centers, and the Interdisciplinary Center for Mathematical and Computational Modeling of Warsaw University for a generous allotment of computer time.

References and Notes

(1) Castleman, A. W. In *Cluster of Atoms and Molecules II*; Haberland, H., Ed.; Springer: Berlin, 1994; p 77.
(2) Anderson, S. R. In *Cluster of Atoms and Molecules II*; Haberland, H., Ed.; Springer: Berlin, 1994; p 241.
(3) Roszak, S.; Leszczynski, J. In *Computational Chemistry: Reviews of Current Trends*; Leszczynski, J., Ed.; World-Scientific: Singapore, 2001; Vol. 6, p 179.
(4) Bieske, E. J.; Dopfer, O. *Chem. Rev.* **2000**, *100*, 3963.
(5) Hiraoka, K.; Katsuragawa, J.; Minamitsu, A.; Ignatio, E. W.; Yamabe, S. *J. Phys. Chem. A* **1998**, *102*, 1214.
(6) Dopfer, O.; Olkhof, R. V.; Maier, J. P. *J. Phys. Chem. A* **1999**, *103*, 2982.
(7) Sullivan, K. O.; Gellene, G. I. *Int. J. Mass Spectrom.* **2000**, *201*, 121.
(8) Gora, R. W.; Roszak, S.; Leszczynski, J. *J. Chem. Phys.* **2001**, *115*, 771.
(9) Roszak, S.; Leszczynski, J. *Chem. Phys. Lett.* **2002**, *323*, 278.
(10) Hiraoka, K.; Mori, T. *Chem. Phys.* **1989**, *137*, 345.
(11) Nizkorodov, S. A.; Spinelli, Y.; Bieske, E. J.; Maier, J. P.; Dopfer, O. *Chem. Phys. Lett.* **1997**, *265*, 303.
(12) Nizkorodov, S. A.; Maier, J. P.; Bieske, E. J. *J. Chem. Phys.* **1995**, *102*, 5570.
(13) Nizkorodov, S. A.; Meuwly, M.; Maier, J. P.; Dopfer, O.; Bieske, E. J. *J. Chem. Phys.* **1998**, *108*, 8964.
(14) Verdes, D.; Linnartz, H.; Botschwina, P. *Chem. Phys. Lett.* **2000**, *329*, 228.
(15) Speck, T.; Linnartz, H.; Maier, J. P. *J. Chem. Phys.* **1997**, *107*, 8706.
(16) Botschwina, P.; Oswald, R.; Linnartz, H.; Verdes, D. *J. Chem. Phys.* **2000**, *113*, 2736.
(17) Meuwly, M.; Bemish, R. J. *J. Chem. Phys.* **1997**, *106*, 8672.
(18) Meuwly, M. *J. Chem. Phys.* **1999**, *111*, 2633.
(19) Meuwly, M.; Nizkorodov, S. A.; Maier, J. P.; Bieske, E. J. *J. Chem. Phys.* **1996**, *104*, 3876.
(20) Kolbuszewski, M. *Chem. Phys. Lett.* **1995**, *224*, 39.
(21) Møller, C.; Plesset, M. S. *Phys. Rev.* **1934**, *46*, 618.
(22) Pople, J. A.; Head-Gordon, M.; Raghavachari, K. *J. Chem. Phys.* **1987**, *87*, 5968.
(23) (a) Krishnan, R.; Binkley, J. S.; Seeger, R.; People, J. A. *J. Chem. Phys.* **1980**, *72*, 650. (b) McLean, A. D.; Chandler, G. S. *J. Chem. Phys.* **1980**, *72*, 5639. (c) Clark, T.; Chandrasekhar, J.; Spitznagel, G. W.; Schlayer, P. v. R. *J. Comput. Chem.* **1983**, *4*, 294.
(24) Woon, D. E.; Dunning, T. H., Jr. *J. Chem. Phys.* **1993**, *98*, 1358.
(25) Kendall, R. A.; Dunning, T. H., Jr.; Harrison, R. J. *J. Chem. Phys.* **1992**, *96*, 6796.
(26) Kumar, A.; Meath, W. J. *Can. J. Chem.* **1985**, *63*, 1616.
(27) Curtis, L. A.; Raghavachari, K.; Pople, J. A. *J. Chem. Phys.* **1993**, *98*, 1293.
(28) Davidson, N. *Statistical Mechanics*; McGraw-Hill: New York, 1962.
(29) Sokalski, W. A.; Roszak, S.; Pecul, K. *Chem. Phys. Lett.* **1988**, *153*, 153.
(30) Jeziorski, B.; van Hemert, M. C. *Mol. Phys.* **1976**, *31*, 713.
(31) Chalasinski, G.; Szczesniak, M. M. *Mol. Phys.* **1988**, *63*, 205.
(32) Gaussian 98 (Revision A.7), Frisch, M. J.; Trucks, G. W.; Schlegel, H. B.; Scuseria, G. E.; Robb, M. A.; Cheeseman, J. R.; Zakrzewski, V. G.; Montgomery, J. A.; Stratmann, R. E.; Burant, J. C.; Dapprich, S.; Millam, J. M.; Daniels, A. D.; Kudin, K. N.; Strain, M. C.; Farkas, O.; Tomasi, J.; Barone, V.; Cossi, M.; Cammi, R.; Mennucci, B.; Pomelli, C.; Adamo, C.; Clifford, S.; Ochterski, J.; Petersson, G. A.; Ayala, P. Y.; Cui, Q.; Morokuma, K.; Malick, D. K.; Rabuck, A. D.; Raghavachari, K.; Foresman, J. B.; Cioslowski, J.; Ortiz, J. V.; Stefanov, B. B.; Liu, G.; Liashenko, A.; Piskorz, P.; Komaromi, I.; Gomperts, R.; Martin, R. L.; Fox, D. J.; Keith, T.; Al-Laham, M. A.; Peng, C. Y.; Nanayakkara, A.; Gonzalez, C.; Challacombe, M.; Gill, P. M. W.; Johnson, B. G.; Chen, W.; Wong, M. W.; Andres, J. L.; Head-Gordon, M.; Replogle, E. S.; Pople, J. A. Gaussian, Inc., Pittsburgh, PA, 1998.
(33) Gora, R. W.; Roszak, S.; Sokalski, W. A.; Leszczynski, J. Jackson State University, 1999, JSU preprint.
(34) Schmidt, M. S.; Baldridge, K. K.; Boatz, J. A.; Elbert, S. T.; Gordon, M. S.; Jensen, J. H.; Koseki, S.; Matsunaga, N.; Nguyen, K. A.; Su, S. J.; Windus, T. L.; Dupuis, M.; Montgomery, J. A. *J. Comput. Chem.* **1993**, *14*, 1347.
(35) Froudakis, G. E.; Fanourgakis, G. S.; Farantos, S. C.; Xantheas, S. S. *Chem. Phys. Lett.* **1998**, *294*, 109.
(36) Hiraoka, K.; Yamabe, S. *Stud. Phys. Theor. Chem.* **1994**, *82*, 399.
(37) Boo, D. W.; Lee, Y. T. *J. Chem. Phys.* **1995**, *103*, 520.